The Canadian Mineralogist
Vol. 37, pp. 1025-1039 (1999)

UPPER THERMAL STABILITY OF TOURMALINE + QUARTZ IN THE SYSTEM $MgO–Al_2O_3–SiO_2–B_2O_3–H_2O$ AND $Na_2O–MgO–Al_2O_3–SiO_2–B_2O_3–H_2O–HCl$ IN HYDROTHERMAL SOLUTIONS AND SILICEOUS MELTS

GABRIELA VON GOERNE[§] AND GERHARD FRANZ

Technische Universität Berlin, FG Petrologie, Sekr. EB 15, 10623 Berlin, Str. des 17.Juni 135, Germany

JEAN-LOUIS ROBERT

CNRS, 1a, rue de la Férollerie, F-45071 Orléans Cedex 2, France

Abstract

The upper thermal stability of Mg–Al tourmaline (Na-bearing and Na-free) in the presence of H_2O, SiO_2, H_3BO_3 and HCl has been investigated experimentally at 200 MPa total pressure between 680° and 850°C as a function of the boron content of the fluid, using conventional hydrothermal cold-seal vessels and an internally heated gas apparatus, with a mixture of synthetic and natural minerals and an HCl-bearing hydrous fluid as starting material. In the Na-free system, breakdown of tourmaline + quartz occurs according to the reaction tur + qtz = crd + sil + B-bearing fluid at $T \geq 750°C$, at B_2O_3 contents in the fluid between ~0.5 and ~9 wt%. In the Na-bearing system, the reaction tur + qtz = crd + melt occurs at $T \geq 730°C$, at B_2O_3 concentrations of ~5 to ~8 wt%. The melt contains ~2 wt% B_2O_3. At lower B_2O_3 concentrations in the hydrous fluid, decomposition according to reaction tur + qtz = crd + ab + B-bearing fluid was observed at ~700°C. The composition of tourmaline changes systematically as temperature increases. In the Na-bearing system, an increasing proportion of vacancies on the *X*-site of tourmaline was found as a result of the substitution $Na_{-1}Mg_{-1}\square Al$, in addition to a certain amount of Al-incorporation by $Mg_{-1}H_{-1}Al$. In the Na-free system, the latter substitution leads to Al-enriched tourmaline.

Keywords: tourmaline + quartz, upper thermal stability, granite system, cordierite, hydrothermal experiments.

Sommaire

Nous avons déterminé la limite supérieure du champ de stabilité de la tourmaline riche en Mg et Al (avec ou sans Na) en présence de H_2O, SiO_2, H_3BO_3 et HCl à une pression de 200 MPa entre 680° et 850°C en fonction de la teneur en bore de la phase fluide. Ces expériences ont été menées avec autoclaves conventionnels à joint froid ou à chauffage interne sur des mélanges de minéraux naturels ou synthétiques et une phase fluide contenant HCl. Dans le système sans sodium, la déstabilisation de l'assemblage tourmaline + quartz se fait selon la réaction tur + qtz = crd + sil + phase fluide borifère à une température égale à ou dépassant 750°C, et à une teneur en bore de la phase fluide comprise entre ~0.5 et 9% (poids). Dans le système avec sodium, la déstabilisation se fait selon la réaction tur + qtz = crd + liquide silicaté à une température minimale de 730°C et à une teneur en bore de la phase fluide comprise entre ~5 et ~8% (poids). Le liquide silicaté contient environ 2% de B_2O_3. A des teneurs inférieures à ce seuil, la déstabilisation se fait selon la réaction tur + qtz = crd + ab + phase fluide borifère à environ 700°C. La composition de la tourmaline change de façon systématique à mesure que la température augmente. Par exemple, dans le système avec sodium, la proportion de lacunes sur le site *X* résulte de la substitution $Na_{-1}Mg_{-1}\square Al$; il y a aussi une certaine mesure d'incorporation d'aluminium selon $Mg_{-1}H_{-1}Al$. Dans le système sans Na, c'est ce dernier schéma qui serait responsable de l'enrichissement de la tourmaline en Al.

(Traduit par la Rédaction)

Mots-clés: tourmaline + quartz, limite supérieure du champ de stabilité, système granitique, cordierite, expériences hydrothermales.

§ *Present address:* Division of Exploration and Mining, CSIRO, P.O. Box 136, North Ryde, NSW 2113, Australia. *E-mail address*: gabriela.vongoerne@dem.csiro.au

Introduction

Tourmaline is a common mineral in granitic rocks, greisen, granitic pegmatites and hydrothermal systems. The upper thermal stability of the assemblage tourmaline + quartz is critical to the question of whether tourmaline has survived as a refractory mineral during melting of a source rock or appeared as a new mineral precipitated from the melt or from a hydrous fluid in these quartz-saturated systems.

The aim of this study is to determine the upper thermal stability in the systems $MgO–Al_2O_3–SiO_2–B_2O_3–H_2O$ and $Na_2O–MgO–Al_2O_3–SiO_2–B_2O_3–H_2O$ in the presence of acid HCl-bearing solutions. These systems may serve as a simplified model for granitic systems. Pressure was kept constant at 200 MPa, a relevant pressure for granitic rocks as well as hydrothermal conditions. We try to answer the following questions: a) What are the breakdown reactions? b) At what temperature does the breakdown start and end? c) At what temperature does the first melt occur? d) What is the composition of the fluid, in terms of its Na and B content and pH?

Background Information

From previous experimental data, the upper thermal stability of dravite, $NaMg_3Al_6(Si_6O_{18})(BO_3)_3(OH)(OH)_3$, and magnesiofoitite (abbreviated as "Mg-foitite", following the tourmaline classification of Hawthorne & Henry 1999), $\square(Mg_2Al)Al_6(Si_6O_{18})(BO_3)_3(OH)(OH)_3$, has been constrained between 700 and 800°C at a pressure between 50 and 500 MPa (Robbins & Yoder 1962, Werding & Schreyer 1984). Werding & Schreyer (1984) showed that in the presence of excess B_2O_3 in the fluid, magnesiofoitite decomposes at 800°C and 200 MPa to grandidierite and one or more unknown phases. Without excess B_2O_3, the upper thermal stability is shifted to 730°C at 100 MPa, and cordierite is the breakdown product of tourmaline, as was also observed by Weisbrod *et al.* (1986), Wolf & London (1997) and von Goerne *et al.* (1997). Al-silicate phases (mullite, B-bearing mullite, sillimanite) have also been observed (Werding & Schreyer 1984, Weisbrod *et al.* 1986). The influence of boron concentration in the fluid on the stability of dravite and cordierite was studied in detail by Weisbrod *et al.* (1986) and Wolf & London (1997).

In a projection from B_2O_3, HCl and H_2O (Fig. 1a), the possibly important phases in the system $MgO–Al_2O_3–SiO_2–B_2O_3–H_2O–HCl$ are shown. Though our experiments were performed in the presence of HCl, the absence of detectable amounts of Cl in most of the solid products indicates that it remains mainly in the fluid phase. The upper thermal stability of the common assemblage tourmaline + quartz may include the minerals cordierite, sillimanite, dumortierite, kornerupine, grandidierite, werdingite and sapphirine. From available experimental data (reviewed by Werding & Schreyer 1996), it can be inferred that B-free and B-bearing kornerupine are probably not stable at 200 MPa, and they are therefore not considered further. Dumortierite breaks down at temperatures slightly above 700°C and 200 MPa to B-bearing mullite and fluid, and is not considered, because tourmaline is still stable at these conditions. Werdingite is a possible product of low-pressure breakdown, but the data of Werding & Schreyer (1992) show that it decomposes to Na-free tourmaline + corundum + grandidierite, *i.e.*, a silica-undersaturated system.

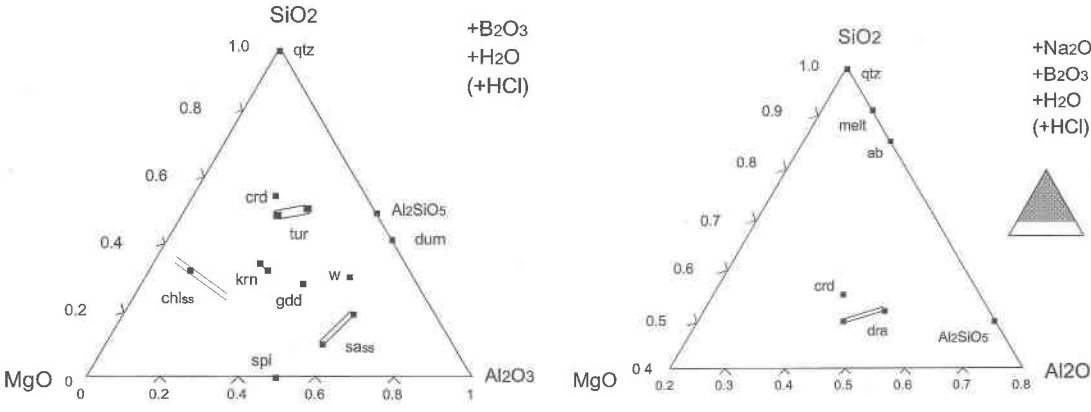

FIG. 1. Selected solid phases of (a) the system $MgO–Al_2O_3–SiO_2–B_2O_3–H_2O$ (+HCl) and (b) the system $Na_2O–MgO–Al_2O_3–SiO_2–B_2O_3–H2O$ (+HCl), projected from B_2O_3 and H_2O. Open symbols: B-bearing phases; Na-free tourmaline and dravite are shown as solid solutions (see text). Abbreviations after Kretz (1983).

Werdingite is therefore neglected here, though one should keep in mind that in natural systems it also occurs together with quartz (Grew & Anovitz 1996). However, the assemblage werdingite + cordierite does not seem to be stable; rather, the assemblage grandidierite + sillimanite appears (Grew & Anovitz 1996), which may justify the decision to neglect werdingite as a first approximation. Grandidierite is a possible breakdown-product of tourmaline because it is stable at 200 MPa in the temperature range between 600°C and 800°C (Werding & Schreyer 1996), as applied in our study.

Synthesis experiments on the end-members magnesiofoitite and dravite (Rosenberg & Foit 1985, Krosse 1995, von Goerne *et al.* 1997) have shown that tourmaline is always enriched in Al compared to the theoretical end-members, and that the composition of tourmaline is a function of temperature (von Goerne *et al.* 1999). We therefore have to consider also a change in chemical composition of tourmaline, mainly a variation in the ratio Al/(Al + Mg) and the *X*-site occupancy, as an important parameter in considerations of the upper thermal stability. This is indicated in Figure 1a by the compositional range of tourmaline as observed in this study.

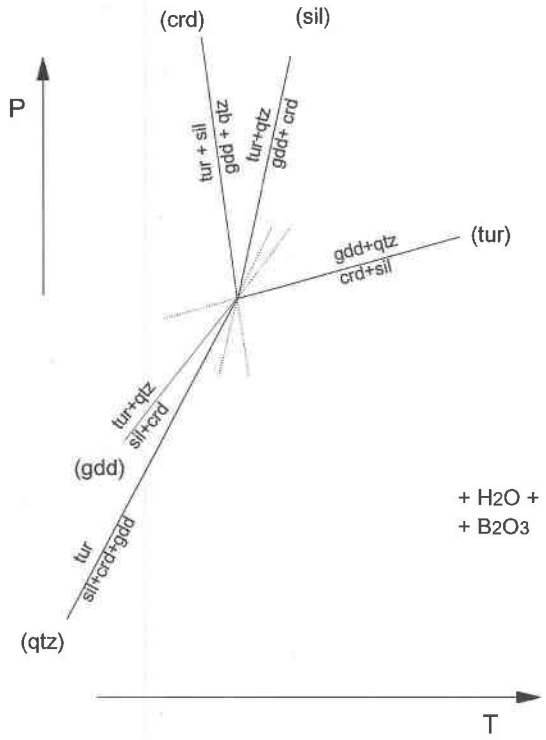

FIG. 2. Phase relations for reactions involving tourmaline, grandidierite, sillimanite, cordierite, quartz and fluid. Fluid-absent reactions are not considered. Tourmaline + quartz is assumed to be the stable low-temperature assemblage, and the equilibrium curve for the decomposition is assumed to have a positive slope.

Our considerations start from the assumption that cordierite + sillimanite, the common assemblage at high-grade metamorphic conditions in the B-free system, will react in the presence of a B-bearing fluid phase to form a B-silicate, either grandidierite or tourmaline. This is analogous to the system Al_2O_3–SiO_2–B_2O_3–H_2O, where kyanite + corundum + B-bearing fluid react to dumortierite (Werding & Schreyer 1996). A Schreinemakers analysis yields the configuration shown in Figure 2, projected from B_2O_3 + H_2O (fluid-absent reactions are not considered). An alternative reaction to the upper stability of tourmaline + quartz is therefore the formation of grandidierite + cordierite. In silica-undersaturated systems, tourmaline may break down to sillimanite, cordierite and grandidierite.

In the system Na_2O–MgO–Al_2O_3–SiO_2–B_2O_3–H_2O (+ HCl), melting must be considered. Weisbrod *et al.* (1986) and Vorbach (1989) showed that the upper stability of dravite is limited by melting reactions between 730° and 750°C at 100 to 400 MPa. Experiments in a granitic system at 750°C and 200 MPa by Wolf & London (1997) established that the equilibrium between tourmaline, biotite, cordierite and melt (± spinel, aluminosilicate or corundum) occurs at ~2 wt% B_2O_3 in strongly peraluminous melts. Figure 1b shows that the most likely breakdown reaction in the system Na_2O–MgO–Al_2O_3–SiO_2–B_2O_3–H_2O (+ HCl) is the formation of cordierite + melt, and in the subsolidus region, it is cordierite + albite + fluid. Dravite is shown as a solid solution according to the experimental results of this study.

Since boron is very mobile during fluid–rock interactions and is partitioned during vapor-phase separation, information about the fluid phase in the presence of tourmaline is of great importance. Therefore, we analyzed the fluid phase for B after completion of the run. Boron is bonded to oxygen in the form of tetrahedral complexes such as $B(OH)_4^-$, or trigonal complexes such as $B(OH)_3$ (Palmer & Swihart 1997). The type of bonding is pH-dependent; a low pH stabilizes trigonal B-complexes, and a high pH stabilizes tetrahedral B-complexes. Tourmaline is stable only at low pH (Morgan & London 1989), so $^{[3]}B$ is assumed to be the dominant species in solution in equilibrium with tourmaline (Palmer *et al.* 1992). Because of the relation of pH and tourmaline, we also tried to vary the pH of the solution, although over a restricted range, between ~3 and 4.

In summary, all the previous experimental data and the phase relations indicate that the upper thermal stability of tourmaline in the presence of quartz is limited by cordierite, sillimanite, albite, siliceous melt and hydrous fluid, and depends strongly on the boron content of the fluid as well as its pH. Grandidierite is a possible breakdown-product also, but only at higher P and T. We therefore examined experimentally the reactions involv-

ing cordierite, sillimanite, albite, siliceous melt and hydrous fluid in the Na-free and Na-bearing system, starting from cordierite + sillimanite + B-fluid and cordierite + albite + B-fluid, respectively (called "backward runs"; see Table 1, run series A and B), from tourmaline + quartz ("forward runs", run series C and D), and from a mixture of the reactant and product assemblage ("equilibrium runs", run series E and F) and determined the boron content in the final fluid by leaching.

Experimental Techniques

Experiments were performed at a constant pressure of 200 MPa using standard cold-seal hydrothermal techniques for experiments at 750°C or less (run duration 10 days). Uncertainties in temperature (measured with Ni–Cr–Ni thermocouples closely adjoining the sample) are estimated to be less than ±5°C, and uncertainties in pressure (measured with a calibrated strain gauge), ±10 MPa. The experiments were quenched by cooling the bombs with compressed air, resulting in a temperature drop of 250°C in the first 5 minutes. For experiments at 800° and 850°C, we used an internally heated pressure vessel mounted vertically, with Ar as the pressure medium (run duration 4 days). Total pressure was recorded continuously with a strain gauge, and the uncertainty is ±2 MPa. Temperature was recorded with a chromel–alumel thermocouple, and the uncertainty is less than ±10°C. Quenching was performed by cooling with Ar, with a drop of 500°C in less than 4 minutes. Gold and platinum capsules (30 mm long, inner diameter 5 mm) were used. Owing to the high temperature of the runs, we assume that $f(O_2)$ was mainly controlled by the autoclave material, near the NNO buffer. The exact proportions of the three different mixtures of starting materials (run series A, C and E; "backward", "forward" and "equilibrium runs", respectively) for reaction (1)

magnesiofoitite + quartz = cordierite + sillimanite + fluid (1)

and the analogous mixtures for reaction (2)

dravite + quartz = cordierite + albite + fluid (2)

(run series B, D and F; "backward", "forward" and "equilibrium runs", respectively) are given in Table 1. Stoichiometric amounts of the powdered solid starting materials were mixed in an agate mortar by hand to homogenize the material. Boron (as solid H_3BO_3) as well as quartz and Na (as NaCl–NaOH solution in the Na-bearing system) were added in 15 mol% excess to prevent loss into the fluid. The fluid:solid ratio for the runs is 1:1. Fluids were added as pure H_2O or HCl, $NH_4(OH)$, NaCl, NaOH solutions (Table 1) to vary the pH of the starting solution. However, owing to the presence of H_3BO_3 in the starting material, which decomposes into boric acid, this range in pH is only on the order of 3.5 to 4.2 (calculated from the dissolution of boric acid at atmospheric conditions).

TABLE 1. STARTING MIXTURES FOR THE HYDROTHERMAL EXPERIMENTS

	Na-free tur	Na-bearing tur	sil	crd	ab	qtz	H_3BO_3	fluid 100 µL	pH
A1)	-	-	20.37	9.02	-	12.74	7.88	H_2O	6.1
A2)	-	-	20.37	49.02	-	12.74	7.88	HCl	2.0
A3)	-	-	20.37	49.02	-	12.74	17.88	$NH_4(OH)$	10
A4)	-	-	20.37	49.02	-	12.74	17.88	HCl	3.2
B1)	-	-	-	56.51	16.94	12.81	13.74	NaCl	6.1
B2)	-	-	-	56.51	16.94	12.81	13.74	NaCl/HCl	2.0
B3)	-	-	-	56.51	16.94	12.81	13.74	NaOH	10
B4)	-	-	-	56.51	16.94	12.81	13.74	NaCl/HCl	3.2
C4)	96.87	-	-	-	-	0.385	2.74	HCl	3.2
D4)	-	75.43	-	-	-	22.33	2.02	NaCl/HCl	3.2
E4)	48.52	-	11.99	28.86	-	1.48	9.15	HCl	3.2
F4)	-	39.44	-	33.29	9.98	10.26	7.04	NaCl/HCl	3.2

Run series A, C and E refer to the Na-free system, run series B, D and F to the Na-bearing system, A and B are backward runs, C and D are forward runs, E and F are equilibrium runs. Weights are given in mg; total solid: 100 mg, total fluid: 100 µL.

After the runs, the capsules were weighed to check for possible leaks. All capsules have lost between 0.74 to 0.98 mg during the experiment, indicating an effective diffusive transport of H_2 during the experiment and thus a control of $f(O_2)$ by the vessel material. The capsules were opened in 50 mL distilled H_2O at 60°C and washed for 10 minutes to dissolve possible B-bearing quench-phases. This method is necessary to get information about concentration of B, Na and pH after the run, though it has the disadvantage that quench phases cannot be observed directly, as precipitates on the capsule wall, for example. The solid was filtered, dried and weighed; from the difference in weight, the amount of fluid remaining at the end of the run was determined. The pH of the 50 mL of solution after cooling to room temperature was measured with an conventional pH-meter and then recalculated to the final fluid of the experiment. Though the pH of the fluid quenched to room temperature is definitely not the same as at run conditions, the quench pH at least monitors relative differences for the runs. Boron as well as Na contents of the final fluids were measured by inductively coupled plasma – atomic emission spectrometry (ICP–AES).

Synthetic and natural minerals served as starting materials. Cordierite was prepared from a gel at 1100°C at atmospheric pressure in 7 days, albite from a gel at 600°C, 100 MPa, 10 days run time with 2 m NaCl solution in excess. Natural quartz and sillimanite come from a sillimanite fels (Meidob Hills, Sudan; personal collection of GvG). All minerals were investigated by X-ray diffraction (XRD) and found to be pure. The unit-cell parameters are given in Table 2.

Dravite (with 1 m NaCl solution and H_3BO_3 in excess) and magnesiofoitite (H_3BO_3 in excess) were prepared from gels, of composition $NaMg_3Al_6(Si_6O_{18})(BO_3)_3(OH)_4$ and $\square(Mg_2Al)Al_6(Si_6O_{18})(BO_3)_3(OH)_4$, respectively, at 600°C, 100 MPa in 10 days run time. The crystals were too small for electron-microprobe (EMP) analysis, as generally observed for tourmaline synthesized by this method. Its composition thus was estimated by comparison of the unit-cell dimensions with published data on tourmaline of known composition, in combination with data generated in this study (Table 2, stars in Fig. 3b). An Al/(Al + Mg) value of 0.7 and 0.8, respectively, can be estimated. The Na-content of the tourmaline in the Na-bearing system is ≥0.92 atoms per formula unit, *apfu* (Table 2).

In addition to optical determinations and examination of run products by scanning electron microscopy (SEM), reaction progress was determined by analyzing the change in intensity of the main peaks in the X-ray powder-diffraction diagram, specifically of (101) of quartz at 3.34 Å, (110) and (222) of cordierite at 8.45 and 3.13 Å, respectively, (210) and (120) of sillimanite at 3.36 and 3.41 Å, respectively, (002) and ($\bar{2}$01) of albite at 3.20 and 4.03 Å, respectively, and (051) and (122) of tourmaline at 2.58 and 2.97 Å, respectively. Additional phases and unit-cell dimensions of tourmaline were calculated from X-ray-diffraction data obtained with a Siemens instrument with Co$K\alpha$ radiation, externally calibrated with Si (NBS 640b) and refined by Rietveld refinement using the GSAS software of Larson & van Dreele (1996). The unit-cell dimensions of tourmaline were refined in space group *R*3*m*, cordierite, in space group *Cccm*, sillimanite, in space group *Pbnm*, and albite, in space group $C\bar{1}$.

Solids were analyzed with an automated Cameca Camebax SX–50 electron microprobe operated in wavelength-dispersion mode, using PAP correction programs. Natural minerals (albite for Na and Si, forsterite for Mg, corundum for Al, danburite for B, vanadinite for Cl) were used as standards. Standard operating conditions were: accelerating potential 15 kV, beam current 12 nA, and 10 seconds counting time. A beam diameter of 2 μm was used. Accuracy approaching ±0.9% relative is obtained. The relative standard error for B lies between 10.7 and 14.2%. For low concentrations such as Na in cordierite or Cl in tourmaline, the relative standard error lies between 7 and 13%, as evaluated from the counting statistics.

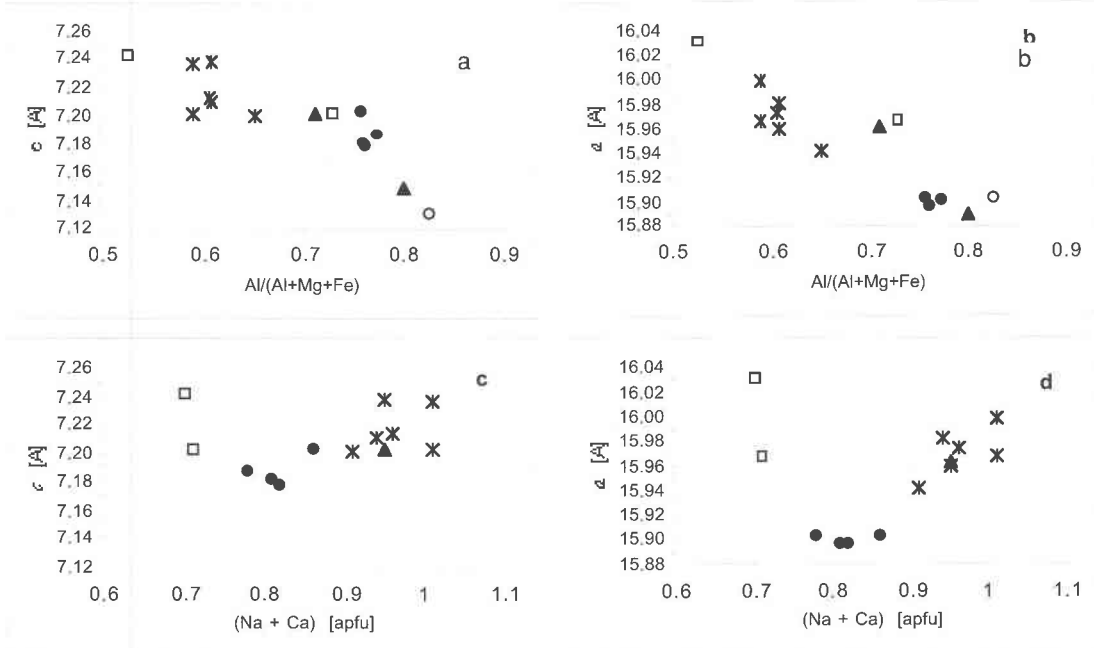

FIG. 3. The ratio Al/(Al + Mg + Fe) (a, b) and (Na + Ca) content (c, d) of synthetic and natural tourmaline as a function of unit-cell dimensions *c* (a, c) and *a* (b, d). Symbols: ○: Na-free tourmaline, ●: Na- bearing tourmaline, natural tourmaline: □: Gasharova et al. (1997), ✳: Grice & Ercit (1993). Unit- cell dimensions of synthetic tourmaline, used as starting material (▲), indicate an Al/(Al + Mg + Fe) value of 0.80 for Na-free tourmaline and 0.72 for Na-bearing tourmaline. The Na content is 0.95 *apfu*.

TABLE 2. UNIT-CELL PARAMETERS OF STARTING MATERIALS (*) AND OF TOURMALINE, EITHER SYNTHETIC OR NATURAL

sample	*a* (Å)	*b* (Å)	*c* (Å)	V (Å³)
* Na-free tourmaline	15.8891(2)		7.1497(3)	1563.16(2)
* dravite	15.9624(2)		7.2021(1)	1585.14(3)
* cordierite	9.7142(3)	17.805(1)	9.3382(2)	1549.50(3)
* sillimanite	7.4846(4)	7.6714(2)	5.7688(3)	331.23(3)
* albite	8.140(3)	12.7891(2)	9.3382(3)	1549.50(3)
A1-680°C	15.9005(4)		7.1212(2)	1559.22(4)
A2-680°C	15.9001(2)		7.1220(1)	1559.24(2)
A3-680°C	15.9005(1)		7.1228(3)	1559.57(2)
C4-680°C	15.900(2)		7.1181(3)	1558.50(3)
B1-680°C	15.9029(4)		7.2029(1)	1577.53(2)
D4-680°C	15.8941(2)		7.1785(4)	1570.45(3)
F4-680°C	15.8976(5)		7.1809(4)	1571.67(5)
A4-715°C	15.8966(2)		7.1212(3)	1558.57(3)
C4-715°C	15.8995(4)		7.1214(3)	1559.08(4)
E4-715°C	15.8980(3)		7.1202(3)	1558.51(4)
B4-715°C	15.8959(3)		7.1782(2)	1570.74(3)
F4-715°C	15.8959(2)		7.1811(3)	1571.37(5)
A1-730°C	15.9024(4)		7.1311(2)	1561.75(4)
C4-730°C	15.8983(1)		7.1321(2)	1561.18(3)
E4-730°C	15.9012(2)		7.1287(3)	1560.95(3)
B2-730°C	15.9049(4)		7.1748(4)	1571.77(5)
B3-730°C	15.9015(5)		7.1867(2)	1573.71(4)
D4-730°C	15.8971(3)		7.1788(1)	1571.11(2)
F4-730°C	15.8996(3)		7.1853(1)	1573.02(4)
C4-750°C	15.8991(4)		7.1268(2)	1558.16(3)
Gasharova	$(Na_{0.21}Ca_{0.44}Mg_{0.05}\square_{0.3})$ $(Mg_{1.39}Fe^{2+}_{0.5}Fe^{3+}_{0.91}Ti_{0.2})$ $(Mg_{0.36}Fe^{3+}_{0.91}Al_{4.73})$ $(Si_{5.92}Ti_{0.08}O_{18})$ $(BO_3)_3$ $O_{1.8}(OH)_{2.2}$			
	16.031		7.242	1611.797
Gasharova	$(Na_{0.64}Ca_{0.41}K_{0.06}\square_{0.29})$ $(Mg_{1.72}Fe^{2+}_{0.12}Fe^{3+}_{0.6}Al_{0.56})$ Al_6 (Si_6O_{18}) $(BO_3)_3$ $O_{2.3}(OH)_{1.7}$			
	15.967		7.202	1590.121
Grice	$(Na_{0.77}Ca_{0.18}\square_{0.05})$ $(Mg_{1.86}Fe^{2+}_{0.7}Fe^{3+}_{0.44})$ $(Fe^{3+}_{0.54}Al_{5.47})$ $(Si_{5.78}Ti_{0.05}O_{18})$ $(BO_{3.17})_3$ $O_{0.4}(OH)_{3.6}$			
	15.960		7.238	1597
Grice	$(Na_{0.55}Ca_{0.35}Li_{0.04}\square_{0.06})$ $(Mg_{2.34}Fe^{2+}_{0.49}Fe^{3+}_{0.17})$ $(Fe^{3+}_{0.44}Al_{5.47})$ $(Si_{5.98}Ti_{0.05}O_{18})$ $(BO_3)_3$ $F_{0.44}O_{0.4}(OH)_{3.21}$			
	15.981		7.210	1595
Grice	$(Na_{0.7}Ca_{0.3}K_{0.01})$ $(Mg_{2.7}Fe^{2+}_{0.31})$ $(Fe^{3+}_{0.69}Al_{5.29})$ $(Si_{5.94}Ti_{0.07}O_{18})$ $(BO_3)_3$ $F_{0.42}O_{0.3}(OH)_{3.28}$			
	15.999		7.236	1604
Grice	$(Na_{0.82}Ca_{0.09}\square_{0.09})$ $(Mg_{2.73}Fe^{2+}_{0.02}Al_{0.25})$ $(Fe^{3+}_{0.03}Al_{5.86})$ $(Si_{5.9}Ti_{0.12}O_{18})$ $(BO_{3.08})_3$ $F_{0.17}O_{0.25}(OH)_{3.58}$			
	15.941		7.201	1585
Grice	$(Na_{0.42}Ca_{0.54}\square_{0.04})$ Mg_5 $(Mg_{0.54}Al_{5.46})$ $(Si_{5.99}Ti_{0.06}O_{18})$ $(BO_3)_3$ $F_{0.69}O_{0.1}(OH)_{3.16}$			
	15.973		7.213	1594
Grice	$(Na_{0.7}Ca_{0.3}K_{0.01})$ $(Mg_{2.7}Fe^{2+}_{0.31})$ $(Fe^{3+}_{0.69}Al_{5.29})$ $(Si_{5.94}Ti_{0.07}O_{18})$ $(BO_3)_3$ $F_{0.42}O_{0.3}(OH)_{3.28}$			
	15.967		7.202	1590.121

Gasharova: Gasharova *et al.* (1997), Grice: Grice & Ercit (1993).

TABLE 3. EXPERIMENTAL RESULTS

sample	run products (XRD)	reaction progress	B_2O_3 (wt% final fluid)	Na_2O (wt% final fluid)	pH	dissol. starting tur (%)	precip. new tur (%)
680°C/200 MPa							
A1	tur, qtz, crd	←	5.03		3.9		45
A2	tur, qtz, crd	←	1.57		4.1		76
A3	tur, qtz, crd ± ?	←	3.19		6.4		62
C4	tur, crd, qtz ± ?	→	2.36		4.1	12	
E4	tur, qtz, crd	←	3.18		4.0		21
B1	tur, qtz, crd	←	2.50	2.84	2.3		47
B2	tur, qtz, crd ± chl	←	3.05	6.83	4.4		42
B3	tur, ab, qtz ± crd	←	4.07	1.93	4.2		33
D4	tur, qtz	↔	1.55	3.18	3.7	30	
F4	tur, qtz ± ab	←	2.40	3.08	4.0		18
715°C/200 MPa							
A4	tur, qtz, crd	←	4.88		4.1		38
C4	tur, crd, qtz	→	1.26		3.6		2
E4	tur, crd, qtz	←	4.19		3.5		33
B4	crd, qtz, tur	←	3.68	3.46	3.4		36
D4	crd, ab, tur, qtz	→	2.00	n.d.	3.7	34	
F4	crd, ab, qtz, tur	↔	4.86	2.15	3.7	8	
730°C/200 MPa							
A1	sil, crd, qtz, tur	←	5.76		3.9		39
A2	crd, sil, qtz, tur	←	1.83		4.6		74
A3	sil, crd, tur, qtz	←	n.d.				
C4	crd, tur, qtz ± ?	→	0.42		3.7		10
E4	crd, sil, tur ± qtz	←	0.43		4.0		10
B1	crd, qtz, melt ± ?	↔	6.51*	10.18	4.5		
B2	crd, melt, qtz	←	7.16*	1.40	4.6		
B3	crd, qtz, tur, melt	←	4.76*	6.27	4.4		
D4	tur, qtz ± ?, ± ab	→	2.80	2.81	4.1	41	
F4	crd, tur, qtz ± ab	→	6.07	7.02	3.8	76	
750°C/200 MPa							
A4	crd, sil, qtz ± tur	←	4.47		4.5		50
C4	crd, sil, tur ± ?	→	7.31		2.9	57	
E4	crd, sil, tur ± qtz	↔	4.65		3.9		8
B4	melt, crd, qtz	↔	5.57*	7.02	2.1		
D4	tur, qtz, ab, ?	→	2.24	3.74	3.5	36	
F4	crd, qtz, melt ± tur	→	7.84*	5.96	3.6		
800°C/200 MPa							
A4	crd, sil, ± qtz	↔	6.23		4.0		(34)
C4	crd, sil, qtz ± tur	→	n.d.				
E4	crd, sil, qtz, tur	→	6.15		3.5	61	
850°C/200 MPa							
A4	sil, crd ± qtz	↔	8.36		3.8		(15)
C4	sil, crd ± qtz, ± tur	→	3.38		4.0	21	
E4	sil, crd ± qtz	→	8.08		3.8	78	

Reaction progress determined by shift of XRD peak intensities (← toward crd + sil or ab, → toward tur + qtz, ↔ no progress). Mass-balance calculation for tourmaline formation or dissolution based on the concentration of B. For runs that yielded melt (*), no mass balance is possible. Starting mixtures: A: sil + crd + qtz, B: crd + ab + qtz, C: Na-free dravite + qtz, D: dravite + qtz, E: Na-free dravite + sil + crd + qtz, F: dravite + crd + ab + qtz. Abbreviations after Kretz (1983): tur: tourmaline, crd: cordierite, ab: albite, sil: sillimanite, chl: chlorite, ?: unidentified phase).

Experimental Results

Na-free system (mixtures A, C, E)

At 680°C, tourmaline (fine-grained aggregates of up to 70 μm in length) and quartz are the major phases (Table 3). All runs contain small amounts of cordierite (Fig. 4a) with a porous surface, and over- and intergrown with tourmaline. Cordierite appears also in the

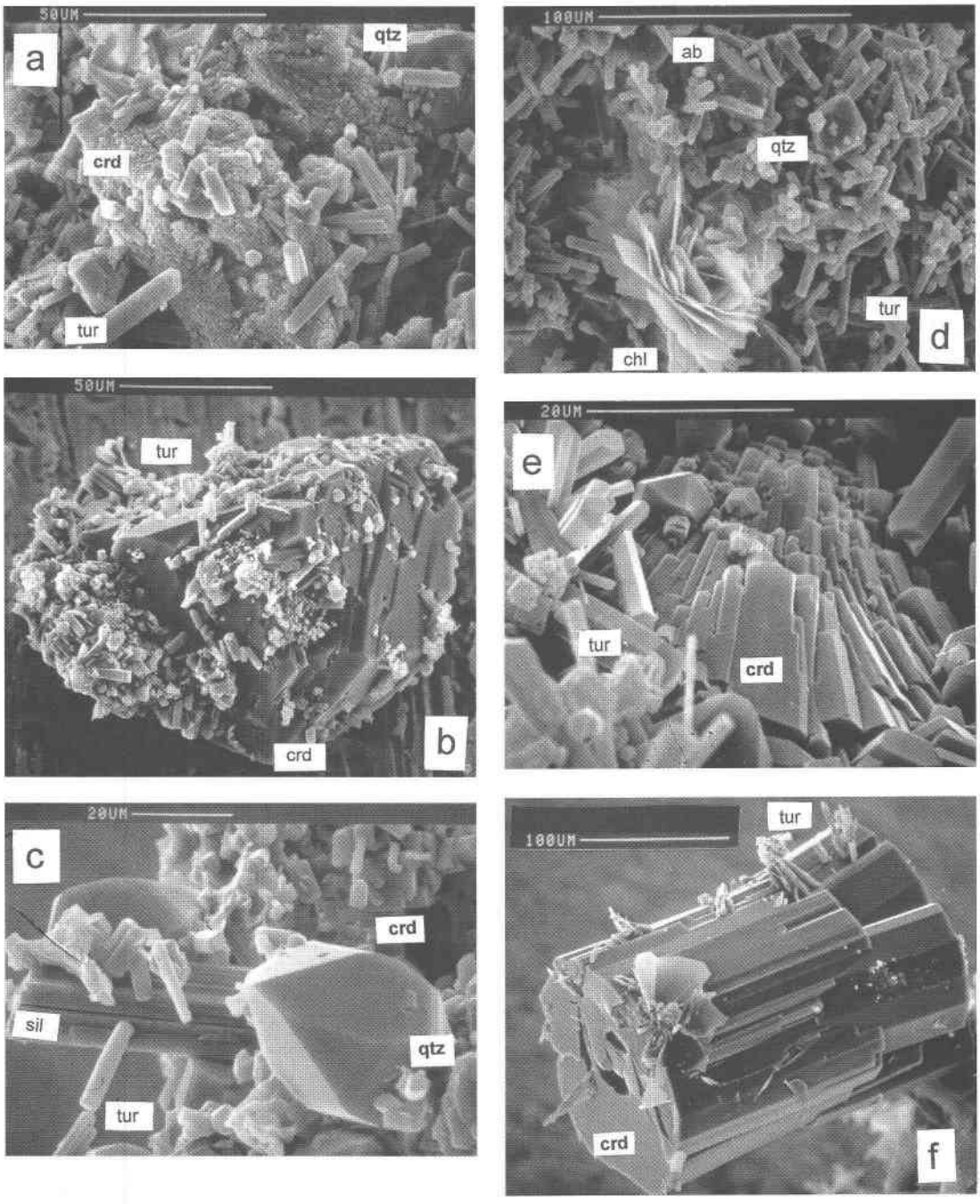

FIG. 4. SEM photo of run products. a. Run A2, 680°C: cordierite with a porous surface is intergrown with and overgrown by tourmaline up to 40 μm in length. b. Run A4, 715°C: well-shaped cordierite up to 280 μm in diameter is overgrown by tourmaline up to 30 μm in length. c. Run A3, 730°C: coexisting tourmaline up to 25 μm in length + sillimanite + quartz + cordierite. d. Run B2, 680°C: tourmaline up to 30 μm in length, albite, quartz, resorbed cordierite and chlorite. e. Run B4, 715°C: tourmaline up to 40 μm in length + cordierite. f. Run D4, 730°C: large crystals of cordierite are intergrown with and overgrown by tourmaline up to 30 μm in length. Abbreviations after Kretz (1983). Scale bars: 20 μm in 4c and 4e, 50 μm in 4a and 4b, and 100 μm in 4d and 4f.

forward run C, which started from tourmaline and quartz only. Sillimanite has disappeared completely, but small amounts of a phase similar to mullite were observed, with main peaks at (210) = 3.40 Å and (110) = 5.40 Å.

At 715°C, tourmaline and quartz are the major phases; they grew as small single crystals or radial aggregates. Cordierite appears in all runs in well-shaped, relatively large crystals up to 280 μm in size (Fig. 4b). Its euhedral faces are overgrown with tourmaline needles. Sillimanite has disappeared completely in all runs, and no other Al-silicate was found.

At 730°C, sillimanite occurs together with tourmaline, quartz and cordierite (Fig. 4c). However, starting from tourmaline + quartz only, a mullite-like phase appeared instead of sillimanite.

At 750°C, small amounts of tourmaline were formed from cordierite and sillimanite in the backward (A) run. Breakdown of tourmaline produced both sillimanite and a mullite-like phase besides cordierite, whereas in the equilibrium run, no significant change of phases was found.

At 800°C, no new tourmaline was observed by X-ray determination, but small amounts of tourmaline are still present in the forward and equilibrium runs.

At 850°C, no tourmaline was found in the equilibrium run. No mullite-like phase was observed.

The results are shown together with the determined B_2O_3 content in the fluid after the run (Table 3) in Figure 5a. It is clear that at B_2O_3 contents exceeding 5 wt% and a T above 750°C, the assemblage cordierite + sillimanite + B-bearing fluid is stable. The small amounts of tourmaline present at 800°C are interpreted to be relict crystals. At 680° and 715°C, the assemblage tourmaline + quartz is stable, as indicated by the disappearance of sillimanite at B_2O_3 contents between 1.75 and 5 wt%. The new formation of cordierite in the forward runs is interpreted to result from an adjustment of the tourmaline toward a more Al-rich composition (see below). At 730°C, the XRD-based determination of reaction progress in the equilibrium run, as well as the formation of new tourmaline in all backward runs, indicate the stability of tourmaline and quartz. Also at 750°C, we found new tourmaline formed from sillimanite + cordierite (but no reaction in the equilibrium run), and therefore we place the upper stability limit of the assemblage tourmaline + quartz slightly above 750°C (Fig. 5a). Most forward runs (label C in Fig. 5a) yielded an unidentified phase, possibly a metastable mullite-like phase similar to those described by Werding & Schreyer (1984); this phase could not be characterized definitively because of its low abundance in the run products. These runs thus do not contribute evidence for the placement of the equilibrium.

In order to check results concerning the reaction progress, we performed a mass-balance calculation using the concentration of boron determined in the final fluid. A decreasing amount of tourmaline should result in an increase in the B content of the fluid (Table 3) and *vice versa*. From the total amount of fluid and the concentration of B, the amount of newly formed or dissolved tourmaline was calculated, assuming that no other B phase is present. This is a questionable method

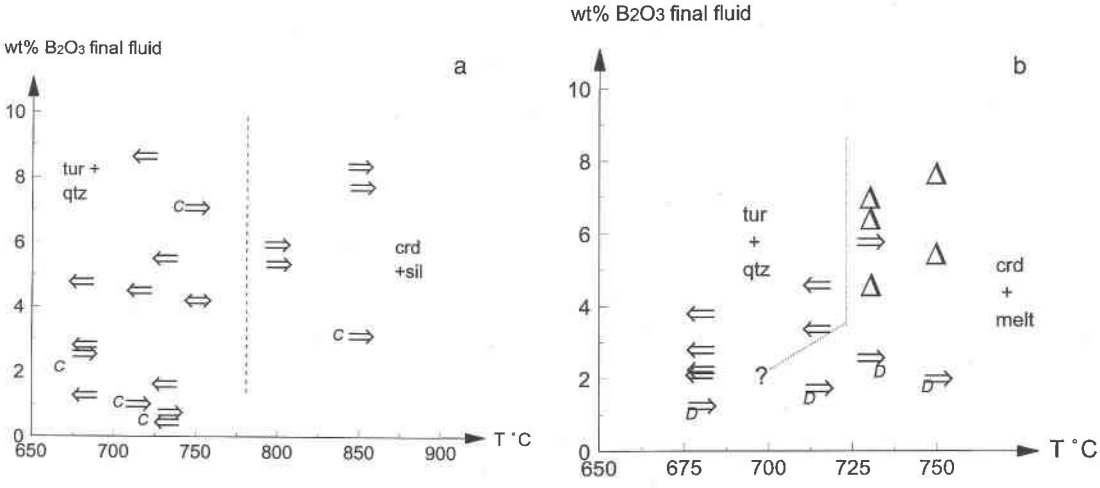

FIG. 5. a. Experimental results for the Na-free system in terms of run temperature *versus* wt% B_2O_3 in the final fluid. Runs labeled "C" (forward runs) started from tourmaline + quartz and yielded unidentified phases. b. Experimental results for the Na-bearing system, in terms of run temperature *versus* wt% B_2O_3 in the final fluid. Runs labeled "D" (forward runs) started from tourmaline + quartz and showed no consistent results. In both cases, the experiments were run at fluid saturation at a pressure of 200 MPa.

for runs in which mullite or similar phases were formed, since these Al-silicates are known to contain B, and it is uncertain how much undissolved quench phases remained in the capsule. We assume that these calculated values of dissolved or newly formed tourmaline are likely to be accurate only above ~10%, but they are consistent with our observations derived from XRD analyses (Table 3) and thus corroborate our interpretation. Figure 6 shows that for the equilibrium runs, there is a systematic, almost linear increase of B_2O_3 content in the final fluid with run temperature; the crossover of the line with the line connecting the starting composition indicates an equilibrium temperature of 770°C.

Na-bearing system (mixtures B, D, F)

At 680°C, tourmaline was formed from cordierite and albite, in both the backward (mixture B) and in the equilibrium runs (mixture F). Depending on the composition of the starting fluid, either small or large amounts of albite are left over; in one case, an additional chlorite-like phase was found (Fig. 4d). In the forward run (mixture D), tourmaline and quartz remained stable.

At 715°C, all runs yielded the same result: the assemblage tourmaline + quartz + cordierite + albite is found, which is a strong indication that this assemblage is stable. The amount of tourmaline is less than at 680°C, and cordierite in grains up to 150 μm across is the dominant phase (Fig. 4e).

At 730°C, the amount of tourmaline is less than 10 vol.%, and cordierite is the major phase (Fig. 4f). In addition, an optically isotropic and clear phase, indicative of a melt, was found in the backward run. No hints for melting could be found in the equilibrium and forward runs. However, tourmaline and quartz did react, because new albite plus an unidentified phase were formed in the forward run.

At 750°C, melt was formed in the backward run from cordierite + albite and in the equilibrium run, where small amounts of tourmaline are still present. The melt forms as isolated clear spheres with a diameter of up to 500 μm and, in some cases, as irregular patches with sharp edges. Again, no melting occurred in the forward run, though the starting assemblage tourmaline + quartz reacted to form albite and an unidentified phase.

The results show a field for cordierite + melt at B_2O_3 contents in excess of 4 wt% and $T \geq 730$°C (Fig. 5b). There is one run where no melt was found; we believe that either small amounts of melt have been overlooked in the sample, or the temperature uncertainty of the run is just within the position of the equilibrium boundary. A field for tourmaline + quartz was found at B_2O_3 contents less than 4 wt% and $T < 730$°C. In combination with the mass-balance calculations of the B_2O_3 contents in the starting and the final fluid (Fig. 6b), the equilibrium temperature was placed at 715 ± 5°C. Owing to the presence of unidentified phases, the discrepancy in the determination of reaction progress by XRD and by

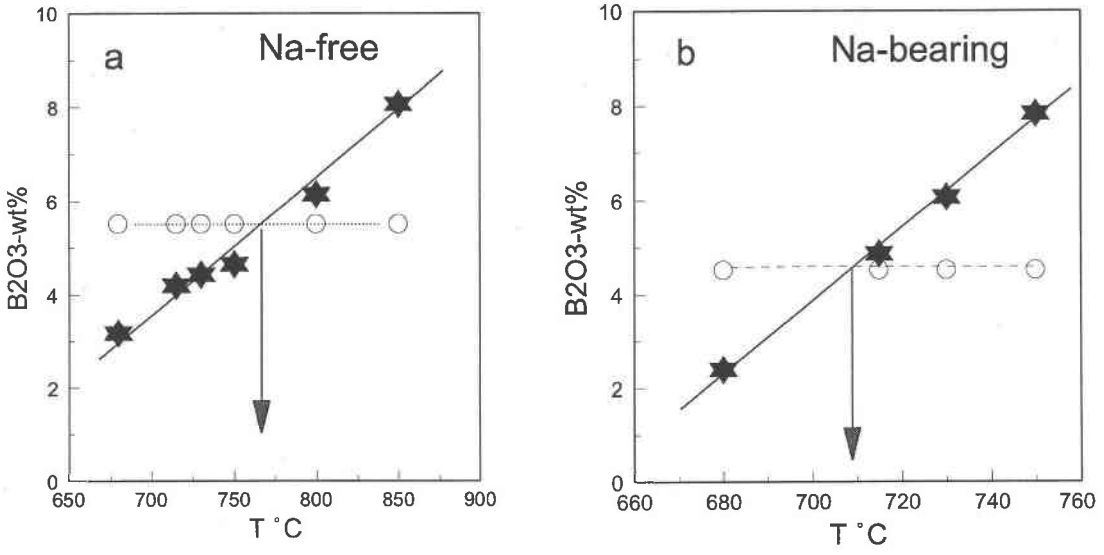

FIG. 6. a. Experimental results of equilibrium runs E and F, in terms of run temperature *versus* wt% B_2O_3 in the starting fluid (○) and in the final fluid (✶). a. Alkali-free system: crossing of the lines of wt% B_2O_3 in starting and final fluid indicate an equilibrium temperature of 775°C. b. Na-bearing system: crossover of the lines of wt% B_2O_3 in starting and final fluid indicates an equilibrium temperature of 710°C.

the mass-balance calculation, and the uncertainty in the unit-cell parameters (see below), products of the forward run (D in Fig. 5b) cannot be interpreted. As in the Na-free system, these results demonstrate that experiments of this type are not useful to determine phase relations in this system.

Composition of Run Products

Tourmaline

Results of EMP measurements of products in all runs that yielded large crystals are shown in Table 4. The compositions differ from the ideal end-members of magnesiofoitite $\square(Mg_2Al)\ Al_6Si_6O_{18}\ (BO_3)_3\ (OH)_4$ and dravite $NaMg_3\ Al_6Si_6O_{18}\ (BO_3)_3\ (OH)_4$ in having higher Al contents and lower calculated (OH) contents: $\square(Mg_{1.5}Al_{1.5})\ Al_6\ (Si_6O_{18})\ (BO_3)_3\ O_{0.5}\ (OH)_{3.5}$ in run A1, 730°C, and $Na_{0.8}\ (Mg_{2.1}Al_{0.9})\ Al_6\ (Si_6O_{18})\ (BO_3)_3\ O_{0.7}\ (OH)_{3.3}$ in run B3, 730°C.

The marked Al-enrichment, with Al up to 7.5 atoms per formula unit (*apfu*), is due to the proton-loss substitution (pls) $Al\square Mg_{-1}H_{-1}$ in the Na-free system and to a combination with the substitution $AlMg_{-1}Na_{-1}$ in the Na-bearing system. In the Na-bearing system, the proportion of vacancies on the *X* site increases slightly with temperature (Fig. 7).

Comparison of the lattice constants of the run-product tourmaline with those of the synthetic starting material shows that in both the Na-bearing and the Na-free systems, lattice constants differ significantly (Fig. 8), indicating that also for those runs where the crystals are too small for EMP analyses, tourmaline did re-equilibrate. In run D4, the cell parameter *c* is excluded from the interpretation.

TABLE 4. ELECTRON-MICROPROBE DATA ON NEWLY GROWN TOURMALINE

sample	B1	B4		F4	A1	B3		D4		
T°C	680°C	715°C		715°C	730°C	730°C		750°C		
SiO_2	37.43	37.94	38.29	38.63	37.79	37.28	37.07	38.08	37.72	36.14	37.30
Al_2O_3	36.24	35.80	37.29	36.27	37.46	36.05	39.07	36.90	37.34	36.55	36.22
MgO	8.96	9.24	8.55	9.53	9.19	9.08	6.58	8.51	8.66	8.02	8.05
Na_2O	2.76	2.78	2.67	2.67	2.71	2.56	0.00	2.54	2.54	2.24	2.37
Cl	0.03	0.00	0.07	0.04	0.00	0.00	0.03	0.02	0.00	0.00	0.00
sum	85.42	85.76	86.87	87.14	87.15	84.97	82.75	86.05	86.26	82.95	83.94
	Cation proportions (*apfu*) based on 15 cations (excluding Na), (OH) calculated by charge balance										
Si	6.00	6.06	6.05	6.06	5.93	5.99	5.98	6.06	5.98	5.95	6.08
Al	6.85	6.74	6.94	6.71	6.93	6.83	7.43	6.92	6.98	7.09	6.96
Mg	2.14	2.20	2.01	2.23	2.15	2.18	1.58	2.02	2.04	1.97	1.96
Na	0.86	0.86	0.82	0.81	0.82	0.80	0.00	0.78	0.78	0.72	0.75
Cl	0.02	0.00	0.02	0.02	0.00	0.00	0.01	0.01	0.00	0.00	0.00
(OH)	3.29	3.28	3.14	3.36	3.37	3.39	3.63	3.18	3.28	3.79	3.13
Al/(Al + Mg)	0.762	0.754	0.775	0.751	0.763	0.759	0.825	0.774	0.773	0.783	0.781

The electron-microprobe data are reported in wt%.

Cordierite

Results of the EMP analysis of cordierite are presented in Table 5. The analytical totals do not reach a sum of 100%, indicating the presence of up to 4 wt% H_2O in the channels of the structure. Na atoms, also located in the channels, reach 0.125 ± 0.06 *apfu* at 715°C, decreasing to 0.094 ± 0.02 *apfu* at 750°C.

Glass

The composition of the glass is summarized in Table 6. It is rhyolitic, with only 0.24–0.50 wt% MgO, slightly increasing with temperature. Na_2O also increases from 1.85 wt% at 730°C to 2.55 wt% at 750°C. The glass is rather homogeneous, except for B_2O_3. The scatter of B-concentrations of approximately ±0.5 wt% between individual spot-analyses in one sample exceeds the precision of the B-determination (± 0.25 wt%). The average B-concentrations are close to 2 wt% B_2O_3 for runs where all tourmaline was consumed, and between 3 and 4 wt% for runs where tourmaline is still present (Table 6). No correlation of B-concentration with other elements could be found. The total of the EMP analysis lies between 88 and 89 wt%, indicating rather constant

TABLE 5. ELECTRON-MICROPROBE DATA ON CORDIERITE PRODUCED BY THE BREAKDOWN OF TOURMALINE

sample	B4	D4		B3	D4	E4	F4
	715°C	715°C		730°C	750°C	750°C	750°C
SiO_2	49.28	50.03	50.75	51.76	50.45	49.91	50.23
Al_2O_3	33.49	34.45	34.43	34.04	33.39	33.57	34.62
MgO	13.04	12.89	13.47	13.29	12.57	13.31	13.51
Na_2O	0.54	0.63	0.72	0.68	0.47	0.01	0.51
Cl	0.00	0.00	0.00	0.07	0.00	0.03	0.01
sum	96.35	98.00	99.37	99.83	96.88	96.83	98.88
	Cation proportions (*apfu*) based on 18 atoms of oxygen						
Si	4.99	4.96	4.98	5.06	5.06	5.02	4.97
Al	4.00	4.03	3.99	3.92	3.96	3.98	4.02
Mg	1.97	1.98	1.97	1.94	1.96	2.00	2.01
Na	0.106	0.125	0.136	0.128	0.092	0.00	0.095
Cl	0.00	0.00	0.00	0.01	0.00	0.00	0.00

The electron-microprobe data are reported in wt%.

TABLE 6. ELECTRON-MICROPROBE DATA ON GLASS

sample	B1-730°C			B3-730°C			B4-750°C			F4-750°C		
SiO_2	71.07	70.89	71.26	71.25	71.86	70.42	70.63	70.91		70.51	70.81	70.37
Al_2O_3	12.55	12.68	12.33	12.44	12.43	12.41	12.29	11.52		12.44	12.74	12.47
MgO	0.27	0.26	0.29	0.27	0.24	0.28	0.32	0.36		0.51	0.50	0.47
Na_2O	1.98	1.95	2.03	1.81	1.88	1.77	2.36	2.48		2.61	2.63	2.59
B_2O_3	2.18	2.20	2.00	3.33	3.00	3.90	2.10	1.90		3.29	2.70	3.80
Cl	0.03	0.03	0.05	0.06	0.08	0.07	0.01	0.05		0.03	0.03	0.04
sum	88.08	88.01	87.96	89.16	89.49	88.85	87.71	87.22		89.39	89.51	89.74

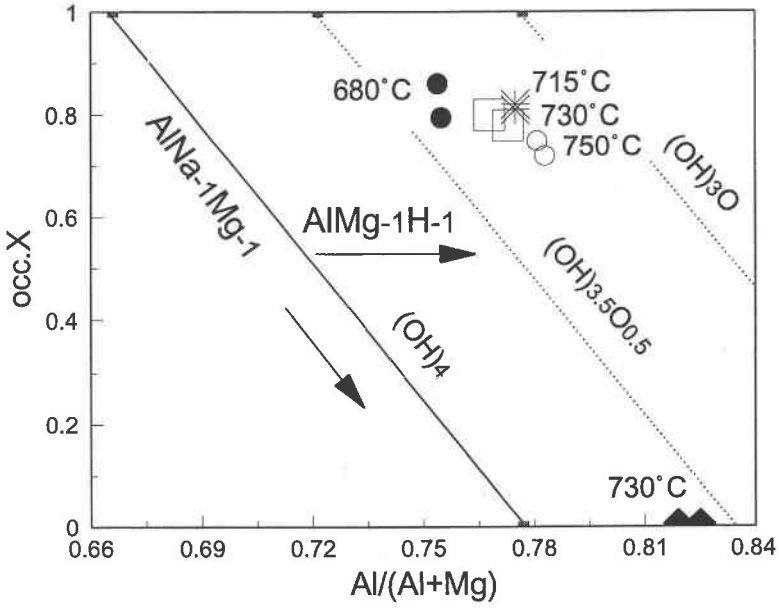

FIG. 7. Composition of tourmaline (results of EMP analyses). The solid line connects end members of ideal dravite – Na-free tourmaline (substitution $Al\square Mg_{-1}Na_{-1}$), and dotted parallel isolines for (OH):O proportion show the effect of the $Al\square Mg_{-1}H_{-1}$ substitution. All tourmaline compositions are enriched in Al compared to the ideal end-members, and in the Na-bearing tourmalines, the proportion of vacancies increases with temperature of the run. Symbols: Na-bearing system (B,D,F): ● (680°C), ✶ (715°C), □ (730°C), ○ (750°C); alkali-free system (run A1, 730°C): ▲; end-members dravite (dra), dravite–dt (dra–dt) and alkali-free dravite (af–dra): ■.

H_2O contents of 11 to 12 wt%. No difference in composition between melt spheres and irregular patches could be observed.

Fluid

After quenching, the boron concentration and the pH of the final fluid were measured (Table 3). All values of pH lie between 2.1 and 6.4, with the majority in the interval 3–4. Calculation of pH of the final solution by dissociation of H_3BO_3 at atmospheric conditions yielded similar results as the measured pH. This indicates that the pH of the fluid is controlled by the boric acid. The boron concentration in the final fluid spans a wide range, from 1.6 to 8.4 wt% B_2O_3. A systematic increase of B with increasing temperature is observed in the equilibrium runs E and F (Figs. 6a, b). The lines cut the B concentration of the starting mixtures at 778°C in the alkali-free system and at 715°C in Na-bearing system. Lower temperatures and B concentrations indicate growth of tourmaline, higher temperatures and B concentrations indicate dissolution of tourmaline.

The Na content of the fluid ranges between 1.9 and 7.1 wt% Na_2O. It is higher where the fluid coexists with melt (*e.g.*, run B4, 750°C, with 6.27 wt% Na_2O) and lower where the fluid coexists with albite (*e.g.*, run F4, 715°C, with 2.15 wt% Na_2O). In every assemblage (fluid – melt – tur – crd, fluid – ab – tur – crd), a systematic increase of Na in the fluid with temperature is ob-

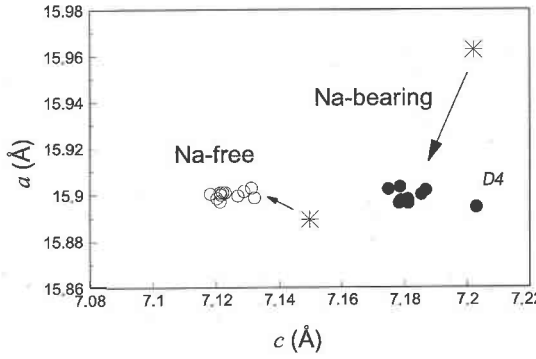

FIG. 8. Unit-cell parameters of synthetic starting tourmaline (✶) compared to the unit-cell parameters of the run-product tourmaline. Symbols: ○: Na-free system, ●: Na-bearing system. Run D4 started from tourmaline + quartz and cannot be interpreted.

served. With increasing Na content in the fluid, the Na contents in tourmaline, cordierite and melt decrease slightly (Fig. 9).

Discussion and Conclusions

The EMP data of the re-equilibrated tourmaline after the runs show that it has a higher Al/(Al + Mg) value than the ideal end-members dravite and magnesiofoitite. The substitution involves mainly the substitutions $AlMg_{-1}H_{-1}$ and $Al\square Mg_{-1}Na_{-1}$ (Fig. 7). Other substitutions, such as $Al_2Mg_{-1}Si_{-1}$ (Tschermaks), are of minor importance (Table 4), as Si is mostly near 6. The change in composition of tourmaline can be described by equilibria (3) and (4) with cordierite in a B-bearing fluid:

Na-free tourmaline$_I$ + quartz + fluid = Na-free tourmaline$_{II}$ + cordierite + B-bearing fluid

$$\square(Mg_2Al_1)\ Al_6\ (Si_6O_{18})\ (BO_3)_3\ (OH)_4 + 1.5\ SiO_2 + 0.65\ H_2O = 0.67\ \square(Mg_{1.5}Al_{1.5})\ Al_6\ (Si_6O_{18})\ (BO_3)_3\ (OH)_{3.5}\ O_{0.5} + 0.5\ Al_3Mg_2\ (Si_5AlO_{18}) + B(OH)_3 + O_2 \quad (3)$$

and

dravite$_I$ + quartz + fluid = dravite$_{II}$ + cordierite + B-bearing fluid

$$NaMg_3\ Al_6\ (Si_6O_{18})\ (BO_3)_3\ (OH)_4 + 0.675\ SiO_2 + 0.8\ H_2O + 1.66\ HCl = 0.3\ Na_{0.8}(Mg_2Al_1)\ Al_6\ (Si_6O_{18})\ (BO_3)_3\ (OH)_{3.2}\ O_{0.8} + 0.975\ Al_3Mg_2(Si_5AlO_{18}) + B(OH)_3 + 0.76\ NaCl + 0.45\ MgCl_2 \quad (4)$$

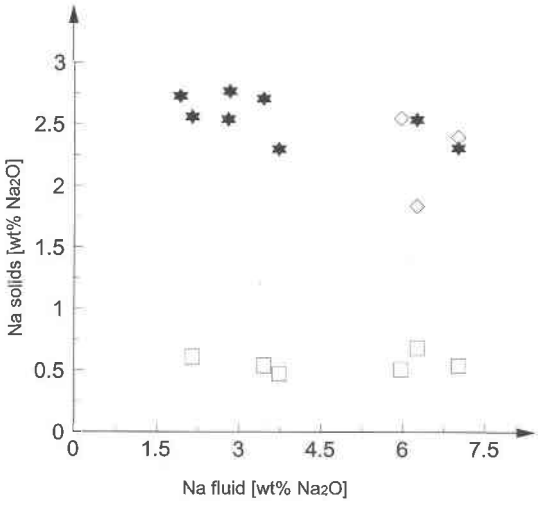

FIG. 9. Na contents (wt% Na_2O) in final fluid and in the solid phases tourmaline (✶), cordierite (□) and melt (◇).

The simplified reaction (3) was written in this way to show that because of the deprotonation of tourmaline, this equilibrium will depend on the $f(O_2)$ of the system. Though in our experiments $f(O_2)$ was not controlled, we assume that at the high temperature of the runs, it was probably buffered by the NNO of the vessel material. Reaction (3) also shows that cordierite buffers the Al/(Al + Mg) ratio of tourmaline (in the presence of quartz and a fluid). Reaction (4) is written with a chloride-bearing solution as used for the experiments, which is probably also a realistic case in nature, since many hydrothermal and magmatic fluids contain Cl, to give an example for such a type of reaction. Reaction (4) clearly shows that the concentration of Na and Mg chlorides (and possibly other species) are important parameters in this equilibrium.

Even at conditions of excess Na in the fluid, the Na content of tourmaline is below the ideal value of 1.0 *apfu*, which is also commonly observed in natural tourmalines, as reviewed by Henry & Dutrow (1996) and London *et al.* (1996). Reaction (4) shows the dependence of the concentration of Na in the fluid, but the experiments also showed (Fig. 9) that cordierite contains considerable amounts of Na, and that albite can be present as an additional phase (which is also a common assemblage for tourmaline in nature). Thus, the Na content of tourmaline will be a function of fluid composition and the solid assemblage, in addition to P and T. From our experiments, we can speculate that dravite with Na = 1.0 *apfu* will be stable at a relatively low temperature, and that with increasing temperature, the proportion of vacancies at the *X* site will increase. This inference is supported by further experimental investigations in the Na-bearing system (von Goerne *et al.* 1999).

In the complex granitic system, Wolf & London (1997) also found synthetic tourmaline with ~0.8 Na *apfu* at an Mg/(Mg + Fe) value of about 0.74, calculated from their Table 5, an indication that this parameter is not strongly influenced by the addition of Fe to the system. However, the Al/(Al + Mg + Fe_{tot}) value of these tourmaline crystals, 0.71, is significantly lower than the values in the range 0.83 to 0.76 reported here. This difference probably results from the fact that a certain amount of Fe will be Fe^{3+}, and thus these values are not strictly comparable.

In addition, all these reactions are a function of the B content in the fluid. Boron is partitioned between the fluid and a solid. At a certain P and T, B will be dissolved in the fluid up to a saturation value, and at higher concentrations a solid phase (*e.g.*, tourmaline) will form. This could be expressed as increasing chemical potential μ_{BO3}^{fluid}, but since we are not able to calculate μ_{BO3}^{fluid} for our experiments, we use simply wt% B_2O_3 plotted against run temperature (at constant pressure of 200 MPa) to represent our results (Fig. 5). Note that this is similar to a T–*X* diagram for mixed-volatile equilibria, the only difference being that for mixed-volatile

equilibria, X is normally expressed as a molar fraction. Since the B-bearing fluid will probably also contain large amounts of Si and other species, it is more convenient to use wt%. Our results for the Na-free system indicate that tourmaline is stable over a large range of B_2O_3 concentrations, between 0.5 and ~9 wt%. They are not compatible with those of Weisbrod *et al.* (1986) for the Na-bearing system, who found a minimum value of ~2 wt% B_2O_3 dissolved in the hydrous fluid, in the presence of tourmaline, cordierite, albite, andalusite and quartz at 100 MPa and 700°C.

The upper thermal stability of Na-free tourmaline can be written as:

$$\text{Na-free dravite}_{ss} + \text{fluid} = \text{cordierite} + \text{sillimanite} + \text{B-bearing fluid}$$

$$\square(Mg_{1.5}Al_{1.5})\ Al_6(Si_6O_{18})\ (BO_3)_3\ (OH)_{3.5}\ O_{0.5} + 2.75\ H_2O = 0.75\ Al_3Mg_2\ (Si_5AlO_{18}) + 2.25\ Al_2SiO_5 + 3\ B(OH)_3 \quad (5)$$

In view of the colinearity of cordierite, sillimanite and tourmaline of this composition (Fig. 1a), the reaction is quartz-absent (*i.e.*, the grandidierite- and quartz-absent reactions in Fig. 2 coincide).

In the Na-bearing system, the upper thermal stability can be written as:

$$\text{dravite}_{ss} + \text{quartz} + \text{fluid} = \text{cordierite} + \text{albite} + \text{B-bearing fluid}$$

$$Na_{0.8}\ (Mg_2Al_1)\ Al_6(Si_6O_{18})\ (BO_3)_3\ (OH)_{3.2}\ O_{0.8} + 2.5\ SiO_2 + 2.9\ H_2O = Al_3Mg_2\ (Si_5AlO_{18}) + 0.8\ NaAlSi_3O_8 + 1.1\ Al_2SiO_5 + 3\ B(OH)_3 \quad (5)$$

Whether the equilibrium temperature for reaction (5) has been reached in our experiments is not clear, because the forward runs ("D" at low concentrations of boron in the fluid; Fig. 5b) produced unidentified phases. However, the reaction boundary as shown in Figure 5b is consistent with the previous results at 100 MPa total pressure by Weisbrod *et al.* (1986). Between 600° and 700°C, they found a strong increase in the concentration of B in the hydrous fluid.

At 730° and 750°C, melting was observed at high concentrations of B in the hydrous fluid. Though the number of experiments for a complete interpretation of the melting behavior as a function of boron concentration, pH and temperature is not sufficient, our results do show that melting starts near 730°C and is favored by high concentrations of boron (Fig. 5b). This also is in agreement with the results of Weisbrod *et al.* (1986), determined at 100–300 MPa total pressure.

The first appearance of melt at ~730°C at 200 MPa is of the same order of magnitude as in the B-free system albite + quartz + fluid = melt (Tuttle & Bowen 1958, Johannes 1980). The relatively small effect of B_2O_3 in the solution, which does not decrease the melting temperature by more than 10 to 20°C, must be due to the extremely refractory behavior of tourmaline and its incongruent melting. This is confirmed by the fact that in the Na-free system, melting was not observed at temperatures up to 850°C, even at 8 wt% B_2O_3 in solution. Werding & Schreyer (1984) also reported that in the presence of excess B_2O_3 in solution, Na-free tourmaline remains stable up to 810°C at 200 MPa.

The high SiO_2 content and constant composition of the glasses (Table 6) indicate the presence of a siliceous melt and not a quench product from a hydrous fluid. The H_2O content of this melt, 11 to 12 wt%, estimated by the wt% difference of the analytical total (EMP analyses) from 100%, is much higher than the H_2O content of a B-free melt at 200 MPa (~7 wt%, measured on a melt of albite or granitic pegmatite composition: Burnham 1979). Similarly high H_2O contents were reported by Wolf & London (1997) in a complex B-bearing granitic system. The absence of melting in the Na-free system, even at 850°C (also observed by Werding & Schreyer 1984), and the similar melting temperatures in the Na-bearing system to the melting of albite + quartz + H_2O, show that the network-forming B does not lower the melting point significantly; instead it can be speculated that the presence of B substantially increases the solubility of H_2O in a felsic melt. However, neither in our experiments nor in those of Wolf & London (1997) is there a clear correlation between B and H_2O content of the glasses. How much H_2O is actually dissolved in the siliceous melt, and how much Si (+ other cations) is dissolved in the hydrous fluid, and where the solvus between the two fluids might eventually close, can only be answered by *in situ* measurements, and must be left open here. It is obvious that there will be severe problems in quenching, even if the quench time of the run could be reduced strongly.

The experimental observation that tourmaline is a liquidus phase is consistent with the widespread occurrence of tourmaline in pegmatite-forming and granitic melts. Tourmaline can be formed by the reaction cordierite + melt = tourmaline + quartz + fluid, or melt = tourmaline + albite + quartz + fluid.

A high concentration of approximately 3 to 5 wt% B_2O_3 in the fluid is required for both reactions, as well as a high concentration of B in the melt. Run products from our experiments that contain tourmaline + melt (Table 3) have B_2O_3 concentrations above approximately 2.3 wt% B_2O_3. Similar results were obtained by Wolf & London (1997) for the complex granitic system. They found that at 750°C, melts with less than 2 wt% B_2O_3, which is the B equivalent of 20 wt% tourmaline in a rock or melt, are still undersaturated in tourmaline, unless the melt is strongly peraluminous. Pichavant *et al.* (1987) observed that in rhyolite with 0.64 wt% B_2O_3, no tourmaline was formed, but the only Mg–Fe mineral is biotite.

Though the assemblage of coexisting cordierite + tourmaline occurs in natural rocks such as the Hercynian

granites of western Europe (*e.g.*, Luxulyan, Cornwall; D. London, pers. commun.), it has not yet been described in detail in the literature. Documentation of their coexistence and of their chemical composition is needed, and we here draw attention to this assemblage. From the distribution of Na between cordierite and tourmaline (Fig. 9), the temperature of crystallization could potentially be inferred (Knop *et al.* 1998). Also, in rocks with plagioclase (albite) + cordierite + sillimanite + tourmaline, the chemical composition of tourmaline in terms of *X*-site occupancy and Al/(Al + Mg) value should be determined and may also give an indication of the temperature of crystallization and the composition of the fluid phase.

Acknowledgements

We kindly acknowledge funding by DAAD, Procope 312/pro-gg. Thanks to F. Holtz and B. Evans for helpful discussions. Technical assistance with electron-microprobe analyses was provided by O. Rouer at BRGM, Orléans. ICP–AES measurements were made at the Université d'Orléans. Hydrothermal synthesis experiments, SEM and XRD investigations were carried out at CRSCM, Orléans. The manuscript greatly benefitted from the constructive review by D. London and E. Grew.

References

Burnham, C.W. (1979): Magmas and hydrothermal fluids. *In* Geochemistry of Hydrothermal Ore Deposits (H.L. Barnes, ed.). Holt, Rinehart and Winston, New York, N.Y. (71-136).

Gasharova, B., Mihailova, B. & Konstantinov, L. (1997): Raman spectra of various types of tourmaline. *Eur. J. Mineral.* **9**, 935-940.

Grew, E.S. & Anovitz, L.M., eds. (1996): Boron: Mineralogy, Petrology and Geochemistry. *Rev. Mineral.* **33**.

Grice, J.D. & Ercit, T.S. (1993): Ordering of Fe and Mg in the tourmaline crystal structure: the correct formula. *Neues Jahrb. Mineral., Abh.* **165**, 245-266.

Hawthorne, F.C. & Henry, D. (1999): Classification of the minerals of the tourmaline group. *Eur. J. Mineral.* **11**, 201-215.

Henry, D.J. & Dutrow, B.L. (1996): Metamorphic tourmaline and its petrologic applications. *Rev. Mineral.* **33**, 503-557.

Johannes, W. (1980): Metastable melting in the granite system Qz–Or–Ab–An–H_2O. *Contrib. Mineral. Petrol.* **72**, 73-80.

Knop, E., Scheikl, M. & Mirwald, P. (1998): Incorporation of sodium into magnesium cordierite below and above the solidus. *Terra Nova, Abstr.* **1**, 30.

Kretz, R. (1983): Symbols for rock-forming minerals. *Am. Mineral.* **68**, 277-279.

Krosse, S. (1995): *Hochdrucksynthese, Stabilität und Eigenschaften der Borsilikate Dravit und Korneruppin sowie Darstellung und Stabilitätsverhalten eines neuen Mg–Al-Borates.* Diss. Ruhr-Universität Bochum, Bochum, Germany.

Larson, A. & van Dreele, R. (1996): *GSAS General Structure Analysis System.* University of California, Los Angeles, California.

London, D., Morgan, G.B., VI & Wolf, M.B. (1996): Boron in granitic rocks and their contact aureoles. *Rev. Mineral.* **33**, 299-330.

Morgan, G.B., VI & London, D. (1989): Experimental reactions of amphibolite with boron-bearing aqueous fluids at 200 MPa: implications for tourmaline stability and partial melting in mafic rocks. *Contrib. Mineral. Petrol.* **102**, 281-297.

Palmer, M.R., London, D., Morgan, G.B., VI & Babb, H. (1992): Experimental determination of fractionation of $^{11}B/^{10}B$ between tourmaline and aqueous vapor: a temperature and pressure dependent isotopic system. *Chem. Geol.* **101**, 123-129.

_____ & Swihart, G.H. (1996): Boron isotope geochemistry: an overview. *Rev. Mineral.* **33**, 709-744.

Pichavant, M., Herrera Valencia, J., Boulmier, S., Briqueu, L., Joron, J.L., Juteau, M., Marin, L., Michard, A., Sheppard, S.M.F., Treuil, M. & Vernet, M. (1987): The Macusani glasses, SE Peru: evidence for chemical fractionation in peraluminous magmas. *In* Magmatic Processes: Physicochemical Principles (B.O. Mysen, ed.). *Geochem.Soc., Spec. Publ.* **1**, 359-373.

Robbins, C. & Yoder, H. (1962): Stability relations of dravite, a tourmaline. *Carnegie Inst. Wash. Yearb.* **61**, 106-108.

Rosenberg, P.E. & Foit, F.F., Jr. (1985): Tourmaline solid solution in the system MgO–Al_2O_3–SiO_2–B_2O_3–H_2O. *Am. Mineral.* **70**, 1217-1223.

Tuttle, O.F. & Bowen, N.L. (1958): Origin of granite in the light of experimental studies in the system $NaAlSi_3O_8$–$KAlSi_3O_8$–SiO_2–H_2O. *Geol. Soc. Am., Mem.* **74**.

von Goerne, G., Franz, G. & Wirth, R. (1999): Synthesis of large dravite crystals by the chamber method. *Eur. J. Mineral.* **11** (in press).

_____, _____ & Heinrich, W. (1997): Experimental calibration of fluid controlled incorporation of sodium in tourmaline. *Int. Symp. on Tourmaline (Brno), Abstr.*, 24.

Vorbach, A. (1989): Experimental examination on the stability of synthetic tourmalines in temperatures from 250°C to 750°C and pressures to 4 kb. *Neues Jahrb. Mineral., Abh.* **161**, 69-83.

WEISBROD, A., POLAK, C. & ROY, D. (1986): Experimental study of tourmaline solubility in the system Na–Mg–Al–Si–B–O–H; applications to the boron content of natural hydrothermal fluids and tourmalinization processes. *Int. Symp. on Experimental Mineralogy and Geochemistry (Nancy), Abstr.*, 140-141.

WERDING, G. & SCHREYER, W. (1984): Alkali-free tourmaline in the system $MgO–Al_2O_3–B_2O_3–SiO_2–H_2O$. *Geochim. Cosmochim. Acta* **48**, 1331-1344.

_____ & _____ (1992): Synthesis and stability of werdingite, a new phase in the system $Mgo–Al_2O_3–B_2O_3–SiO_2$ (MABS), and another new phase in the ABS-system. *Eur. J. Mineral.* **4**, 193-207.

_____ & _____ (1996): Experimental studies on borosilicates and selected borates. *Rev. Mineral.* **33**, 117-163.

WOLF, M. & LONDON, D. (1997): Boron in granitic magmas: stability of tourmaline in equilibrium with biotite and cordierite. *Contrib. Mineral. Petrol.* **130**, 12-30.

Received May 24, 1998, revised manuscript accepted June 1, 1999.